

1 **Carbon limitation leads to thermodynamic regulation of aerobic metabolism**

2 Vanessa A. Garayburu-Caruso<sup>1</sup>, James C. Stegen<sup>1</sup>, Hyun-Seob Song<sup>1,2</sup>, Lupita Renteria<sup>1</sup>,  
3 Jaqueline Wells<sup>1,3</sup>, Whitney Garcia<sup>1</sup>, Charles T. Resch<sup>1</sup>, Amy Goldman<sup>1</sup>, Rosalie Chu<sup>4</sup>, Jason  
4 Toyoda<sup>4</sup>, Emily B. Graham<sup>1\*</sup>

5

6 <sup>1</sup>Pacific Northwest National Laboratory, Richland WA 99352, USA

7 <sup>2</sup>University of Nebraska-Lincoln, Lincoln NE 68588, USA

8 <sup>3</sup>Oregon State University, Corvallis, OR 97331, USA

9 <sup>4</sup>Environmental Molecular Sciences Laboratory, Richland WA 99352, USA

10 \*Correspondence: [emily.graham@pnnl.gov](mailto:emily.graham@pnnl.gov); 509-372-6049

11

12

13 **Abstract**

14 Organic matter (OM) metabolism in freshwater ecosystems is a critical source of uncertainty in  
15 global biogeochemical cycles, yet aquatic OM cycling remains poorly understood. Here, we  
16 present the first work to explicitly test OM thermodynamics as a key regulator of aerobic  
17 respiration, challenging long-held beliefs that organic carbon and oxygen concentrations are the  
18 primary determinants of respiration rates. We pair controlled microcosm experiments with  
19 ultrahigh-resolution OM characterization to demonstrate a clear relationship between OM  
20 thermodynamic favorability and aerobic respiration under carbon limitation. We also  
21 demonstrate a shift in the regulation of aerobic respiration from OM thermodynamics to nitrogen  
22 content when carbon is in excess, highlighting a central role for OM thermodynamics in aquatic  
23 biogeochemical cycling particularly in carbon-limited ecosystems. Our work therefore  
24 illuminates a structural gap in aquatic biogeochemical models and presents a new paradigm in  
25 which OM thermodynamics and nitrogen content interactively govern aerobic respiration.

26

27

28 Metabolism of organic matter (OM) in freshwater ecosystems plays a large role in global  
29 biogeochemical cycles<sup>1-3</sup>, as freshwater ecosystems emit more than 2 Pg C yr<sup>-1</sup> into the  
30 atmosphere<sup>4,5</sup>. These emissions are largely dominated by contributions from river corridors<sup>1,5,6</sup>,  
31 and within the river corridor, areas of groundwater-surface water mixing (hyporheic zones) have  
32 a disproportionate impact on aerobic respiration<sup>7-9</sup>. Recent field observations have suggested that  
33 OM chemistry, and in particular OM thermodynamics, are key to predicting aerobic respiration  
34 in hyporheic zones<sup>10-12</sup>. If supported, these observations challenge a widespread paradigm that  
35 organic carbon and oxygen concentrations are the primary determinants of aerobic respiration  
36 rates and highlight a key source of model uncertainty. Yet, no work has provided direct evidence  
37 for OM thermodynamics as a regulator of aerobic respiration in a controlled laboratory  
38 environment. Demonstrating this behavior would identify mechanisms that drive field-based  
39 phenomena and would enable key properties of OM to be represented in predictive models,  
40 thereby contributing to reducing the uncertainty in modeling river corridor biogeochemical  
41 cycling<sup>13,14</sup>.

42 We use highly controlled aerobic microcosms, non-invasive dissolved oxygen consumption  
43 rates, and ultrahigh-resolution OM characterization to investigate the role of OM chemistry in  
44 determining aerobic respiration in hyporheic zone sediments. Based on field observations<sup>10-12</sup>,  
45 we hypothesized that OM chemistry, including thermodynamic favorability and nitrogen (N)  
46 content, would regulate aerobic respiration. Historically, investigations of thermodynamic  
47 constraints on microbial metabolism have primarily focused on oxidation-reduction reactions  
48 that are controlled by the availability of various terminal electron acceptors (e.g., oxygen, nitrate,  
49 sulfate)<sup>15-17</sup>. Theory indicates that respiration under aerobic conditions is governed by rate  
50 kinetics, while thermodynamic regulation has no influence. This expectation is based on the

51 premise that using oxygen as the terminal electron acceptor provides sufficient energy for ATP  
52 generation regardless of thermodynamic properties of the electron donor<sup>18,19</sup>. Consequently, the  
53 role of OM thermodynamics in microbial metabolism has been mainly explored under anaerobic  
54 conditions<sup>20-23</sup>. However, OM chemistry has recently emerged as a possible regulator of aerobic  
55 metabolism based on correlative field-based observation. These studies have suggested that OM  
56 thermodynamics interact with N content and carbon concentration to influence aerobic  
57 respiration<sup>10-12</sup>. Here, we present the first work to explicitly test OM thermodynamics as a key  
58 regulator of aerobic respiration and demonstrate a clear relationship between OM  
59 thermodynamic favorability and aerobic respiration under carbon limitation, thus challenging  
60 long-held beliefs that respiration rates are govern solely by kinetics.

### 61 **Thermodynamic regulation of aerobic respiration**

62 To test the role OM chemistry as a key regulator of aerobic metabolism, we incubated sediments  
63 with thermodynamically distinct N-bearing or N-free OM treatments at concentrations  
64 commonly observed in freshwater systems (from 0.3 to 9 mg C L<sup>-1</sup>, Supplementary Table  
65 1)<sup>12,24,25</sup>. We inferred carbon limitation at low treatment concentrations (< 3 mg C L<sup>-1</sup>) because  
66 sediments were collected from a low carbon area (%C < 0.6 as previously discussed in Graham  
67 et al.<sup>11</sup>) with observed C:N < 5<sup>11</sup> which is typically associated with carbon limitation<sup>26,27</sup>. In  
68 addition, sediments were pre-processed prior to incubation until dissolved organic carbon  
69 concentrations were below instrument detection (see Methods and Supplementary Fig. 1).  
70 Moreover, aerobic respiration increased with treatment concentration from 0.3 to 3 mg C L<sup>-1</sup> and  
71 stabilized between 3 and 9 mg C L<sup>-1</sup>, indicating that additional carbon only stimulated respiration  
72 when 3 mg C L<sup>-1</sup> or less was amended (Fig. 1a,  $p = 0.005$  &  $p = 0.43$ ).

73

74 We provide direct evidence for OM thermodynamics in controlling aerobic respiration by  
75 demonstrating that thermodynamically-favorable OM supported enhanced respiration in  
76 microcosms under carbon limitation. We use the mean Gibbs free energy of the half reaction of  
77 organic carbon oxidation under standard conditions ( $\overline{\Delta G^{\circ}_{\text{Cox}}}$ ) as a proxy for thermodynamic  
78 favorability throughout this paper, as per LaRowe and Van Cappellen<sup>28</sup>, Graham et al.<sup>11</sup>, and  
79 Stegen et al.<sup>12</sup>. Aerobic respiration was negatively correlated with  $\overline{\Delta G^{\circ}_{\text{Cox}}}$  when OM was  
80 amended at low concentrations (Fig. 1b-c 0.3 mg C L<sup>-1</sup> R<sup>2</sup> = 0.23 *p* = 0.03, 3 mg C L<sup>-1</sup> R<sup>2</sup> = 0.34  
81 *p* = 0.007).

82 While our results support previous field observations that emphasize the role of OM  
83 thermodynamics in predicting aerobic respiration<sup>11,12</sup>, we uniquely underscore the central role for  
84 OM thermodynamics in the metabolism of carbon-limited ecosystems using highly controlled  
85 laboratory experiments. A field study by Graham et al.<sup>11</sup> showed that thermodynamically  
86 favorable OM was preferentially metabolized in sediments across a vegetation gradient.  
87 Similarly, Stegen et al.<sup>12</sup> highlighted the importance of OM thermodynamics in regulating  
88 aerobic respiration within hyporheic zones. While the previous works are based on correlative  
89 observations, our controlled laboratory microcosms allowed us to clearly demonstrate  
90 thermodynamic regulation of aerobic metabolism and define the conditions under which OM  
91 thermodynamics provide an avenue for improving aquatic biogeochemical models.

92 Specifically, we reveal a dependency of thermodynamic OM regulation on organic carbon  
93 concentration, as sediments putatively not experiencing carbon limitation had no evidence of  
94 thermodynamic constraints on aerobic respiration (Fig. 1d, 9 mg C L<sup>-1</sup> *p* = 0.71). Low molecular  
95 weight carbon compounds, such as the amino and organic acids used for treatments in this  
96 experiment (see Methods), are highly bioavailable to microorganisms which have direct uptake

97 pathways for these molecules<sup>29-31</sup> in contrast to polymeric OM in sediments that requires the  
98 production of extracellular enzymes<sup>32,33</sup>. Thus, we hypothesize that excess low molecular weight  
99 and highly bioavailable OM diminishes the benefits of thermodynamic preference in metabolism,  
100 because the low microbial cost of direct uptake outweighs the energy benefit gained from  
101 selective carbon metabolism.

## 102 **Pathways of OM metabolism vary with thermodynamic control of aerobic respiration**

103 We underscore a need for improved model structures for predicting aerobic respiration, as we  
104 observed different metabolic processes between carbon-limited and carbon-replete environments.  
105 To investigate metabolic processes involved in aerobic respiration, we calculated inferred  
106 biochemical transformations in ultrahigh-resolution OM profiles following procedures described  
107 previously<sup>10-12,34-36</sup>. This method relies on the mass accuracy of Fourier transform ion cyclotron  
108 resonance mass spectrometry (FTICR-MS) and produces a count of the number of times a  
109 specific molecule (e.g., glucose, valine, glutamine, etc.) is putatively gained or lost in reactions  
110 (see Methods).

111 While previous work has suggested both thermodynamic and N-related regulation of aerobic  
112 respiration<sup>10-12</sup>, we postulate a carbon limitation threshold beyond which thermodynamic  
113 controls do not persist. Our data suggest that beyond this threshold (i.e., in the absence of carbon  
114 limitation), aerobic respiration is coupled to organic N metabolism. We found no differences in  
115 OM chemistry (Supplementary Fig. 2a-b, all  $p > 0.05$ ), respiration rates ( $p = 0.11$  at  $0.3 \text{ mg C}$   
116  $\text{L}^{-1}$  and  $p = 0.24$  at  $3 \text{ mg C L}^{-1}$ ) or biochemical transformations (Fig. 2a-b,  $0.3 \text{ mg C L}^{-1}$   $p =$   
117  $0.67$ ,  $3 \text{ mg C L}^{-1}$   $p = 0.91$ ) across microcosms with N-bearing vs. N-free OM amended when  
118 respiration was thermodynamically-controlled (i.e., in carbon limited conditions). However,  
119 respiration in carbon-replete microcosms ( $9 \text{ mg C L}^{-1}$ ) increased with the addition of organic N

120 relative to N-free OM, and pathways of OM metabolism varied between treatments with or  
121 without added organic N (Fig. 2c-d,  $p = 0.04$ ,  $p = 0.04$ ). Biochemical transformations in  
122 microcosms receiving  $9 \text{ mg C L}^{-1}$  more frequently involved N when organic N was added to  
123 microcosms (Supplementary Fig. 3,  $p = 0.02$ ). Additionally, we provide evidence that N-  
124 enriched molecules are preferably consumed in natural environments with surplus carbon.  
125 Bioavailable organic N addition increased the relative abundance of more complex protein-like  
126 OM, suggesting the preservation of sediment-bound OM containing N in the presence of more  
127 accessible N sources (Supplementary Fig. 2c,  $p < 0.01$ ). Together, these results are consistent  
128 with N-mining observed previously in this system, whereby OM is oxidized for microbial  
129 acquisition of  $\text{N}^{10,37}$ .

130 More broadly, we highlight that when organic carbon is in excess, there is a dependency of  
131 aerobic respiration on specific nutrient limitations rather than on OM thermodynamics.  
132 Therefore, OM thermodynamics appear to be most informative of aquatic biogeochemistry  
133 within carbon-limited ecosystems, while N availability governs aerobic respiration at higher  
134 carbon to nitrogen ratios (C:N). While N-dependent aerobic respiration at high C:N is consistent  
135 with nutrient limitations observed in variety of systems<sup>38,39</sup>, thermodynamic regulation at low  
136 C:N ratios challenges the widespread notion that organic carbon and oxygen concentrations are  
137 the main variables driving respiration.

### 138 **Enhancing model predictions with a new paradigm of aquatic biogeochemical cycling**

139 While many processed-based models represent biogeochemical cycles, most model structures  
140 contain only a few lumped carbon pools that do not fully represent the complexity of natural OM  
141 sources<sup>20,21</sup>. Organic matter cycling is typically modeled following Michaelis-Menten kinetics,  
142 with OM separated into particulate or dissolved pools<sup>40</sup>. In some cases, these pools are further

143 categorized by environmental properties or bioavailability, and each subpool is assigned a fixed  
144 mineralization rate<sup>20,40-42</sup>. These traditional approaches do not address OM chemistry because  
145 commonly used bulk characterization techniques do not provide sufficient molecular detail, and  
146 because representing individual OM molecules in a given ecosystem is computationally  
147 unfeasible. Our work demonstrates that processes associated with OM thermodynamics and N  
148 content strongly influence aerobic respiration—and, in turn, biogeochemical reaction networks—  
149 thus providing a link between OM chemistry and biogeochemical rates that will help inform and  
150 parameterize new and existing models.

151 We therefore propose a new conceptual model with direct avenues for model incorporation in  
152 which OM thermodynamics regulates aerobic respiration until organic carbon concentrations are  
153 sufficient to induce nutrient limitations (Fig. 3). We suggest that a combination of organic carbon  
154 concentration and thermodynamic limitation governs aerobic respiration in sediments with low  
155 carbon to nutrient ratios. In contrast, nutrient limitation regulates respiration when bioavailable  
156 carbon is in excess, and in this scenario, organic N may be a key constraint on respiration. This is  
157 consistent with previous reports of a strong role from organic N cycling in hyporheic zones and  
158 freshwater systems<sup>10,12,43,44</sup>. While our work represents a single system, our conceptual model is  
159 meant to provide proof-of-concept for more spatially extensive studies that will allow broader  
160 transferability.

161 To our knowledge, this is the first work to provide direct evidence for OM thermodynamics as a  
162 regulator of aerobic respiration in a controlled laboratory environment and highlights a key gap  
163 in current mechanistic understanding of OM cycling. In order to improve model accuracy, we  
164 reveal a need to explicitly represent the interactions between OM thermodynamics, nutrient  
165 limitations, and organic carbon concentration in process-based models of aquatic carbon cycling.



166 Our results constrain the environments under which specific chemical attributes of OM are  
167 valuable for rate predictions and provide guidance on the data types that are needed to accurately  
168 represent hyporheic zone biogeochemistry. These processes cannot be represented by lumped  
169 OM pools informed by decades of coarse measurements, and thus we highlight the utility of  
170 high-resolution technologies in models of aquatic biogeochemistry and present a new paradigm  
171 in which aerobic respiration is governed by a combination of carbon concentration, OM  
172 thermodynamics, and nutrient limitations.

### 173 **Acknowledgements**

174 This research was supported by the U.S. Department of Energy (DOE), Office of Biological and  
175 Environmental Research (BER), as part of Subsurface Biogeochemical Research Program's  
176 Scientific Focus Area (SFA) at the Pacific Northwest National Laboratory (PNNL). Data were  
177 generated under EMSL user proposal 51180. A portion of the research was performed at  
178 Environmental Molecular Science Laboratory User Facility. PNNL is operated for DOE by  
179 Battelle under contract DE-AC06-76RLO 1830.

### 180 **Author Contributions**

181 V.G.C., E.B.G, H.S.S. and J.C.S., conceptualized the study; V.G.C., L.R., J.W., W.G, and A.G.,  
182 carried out the study; C.T.R., R.C. and J.T. conducted instrumental analyses; V.G.C. and E.B.G  
183 drafted the manuscript and all authors contributed to the writing.

### 184 **Competing interests**

185 The authors declare no competing financial interests.

## 186 **Materials and methods**

### 187 **Study site and sediment collection**

188 This study was conducted using sediments from the Columbia River hyporheic zone within the  
189 Hanford Site 300 Area (approximately 46° 22' 15.80"N, 119° 85 16' 31.52"W) in eastern  
190 Washington, USA<sup>10,11,45</sup>. Hyporheic zone sediments were collected in April 2018 at five  
191 locations, separated by ~2 m (depth: ~30 cm). Sediments were sieved in the field to < 2 mm,  
192 homogenized, and kept on ice until same-day laboratory processing. We performed sequential  
193 organic carbon extractions with synthetic river water (see Supplementary Methods for  
194 composition) prior to incubations to minimize the influence of carbon mobilized from sediments  
195 during field sampling. Details regarding pre-processing step are provided in the Supplementary  
196 Methods.

### 197 **Laboratory Microcosms**

198 We used a total of 85 microcosms in a full factorial design (a) four chemically distinct OM  
199 amendments at three concentrations, (b) four autoclaved controls (heat kills), and (c) one  
200 synthetic water control, each treatment with five replicates. Incubations were performed over the  
201 course of 5 days, where each day we incubated 17 bioreactors (i.e., 1 replicate treatment per day,  
202 see design in Supplementary Table 1). On the day prior to the experiment, 10 g of pre-processed  
203 sediments were removed from 4°C storage and subsampled into 20 mL borosilicate glass vials.  
204 Vials were left in the dark at ambient laboratory temperature for 8 h before incubation to  
205 acclimate to room temperature.  
206 To initiate microcosms, 18 mL of treatment solution was added to vials containing sediment,  
207 leaving <1 mL headspace. Treatment solution consisted of synthetic river water and the specific

208 OM compound at the desired concentration (Supplementary Table 1). Nitrate and phosphate  
209 were added to the synthetic river water to provide sufficient nutrients for the duration of the  
210 experiment - nitrate concentration matched ambient groundwater while phosphate concentration  
211 matched the Redfield ratio relative to groundwater N (16N:P). We added the following 4 types of  
212 OM because their thermodynamic properties encompassed the extremes experienced by the  
213 surface and the groundwater in situ<sup>12</sup> and were either N-bearing or N-free: Lysine (Gibbs free  
214 energy of the half reaction of organic carbon under standard conditions,  $\Delta G^{\circ}_{\text{COX}} = 79.40 \text{ kJ (mol C)}^{-1}$ , N-bearing), Serine ( $\Delta G^{\circ}_{\text{COX}} = 41.21 \text{ kJ (mol C)}^{-1}$ , N-bearing), Propionate ( $\Delta G^{\circ}_{\text{COX}} = 79.40 \text{ kJ (mol C)}^{-1}$ , N-free), and Ascorbate ( $\Delta G^{\circ}_{\text{COX}} = 41.21 \text{ kJ (mol C)}^{-1}$ , N-free). The vials were placed  
217 horizontally on a shaker at 250 rpm in the dark at  $21 \pm 1 \text{ }^{\circ}\text{C}$  for the duration of the experiment,  
218 except during dissolved oxygen measurements.

## 219 **Respiration rates**

220 Dissolved oxygen (DO) concentration ( $\mu\text{mol L}^{-1}$ ) was measured in each microcosm every hour  
221 for 6 h using 0.5 cm diameter factory-calibrated oxygen sensors and an oxygen optical meter  
222 (Fibox 3; PreSens GmbH, Regensburg, Germany). The DO measurements were automatically  
223 corrected for temperature and the data were recorded using PST3v602 software (PreSens  
224 GmbH). Respiration rates were calculated as the slope of the linear regression between DO  
225 concentration and incubation time for each microcosm (Supplementary Fig. 4-6). We infer that  
226 changes in DO were driven by aerobic respiration, as DO in heat kills did not change during the  
227 incubation (Supplementary Fig. 7). pH measurements were also collected using an optical meter  
228 and factory calibrated pH sensor spots (pH-1 mini; PreSens GmbH). pH values did not change  
229 during the incubation (Supplementary Fig. 8). After 6 hours, microcosm contents were  
230 transferred to 50 mL sterile polypropylene centrifuge tubes and centrifuged for 5 min at 3200 ref

231 and 20°C. The supernatant was filtered through a 0.22 µm polyethersulfone membrane filter  
232 (Millipore Sterivex, USA) frozen at -20°C until further analysis.

### 233 **Fourier transform ion cyclotron resonance mass spectrometry (FTICR-MS)**

234 Fourier transform-ion cyclotron resonance mass spectrometer (FTICR-MS) (12 Tesla (12T)  
235 Bruker Solarix, Billerica, MA) located at the Environmental Molecular Sciences Laboratory in  
236 Richland, WA, was used to collect high-resolution mass spectra of the OM. Resolution was  
237 220K at 481.185 m/z. The FTICR-MS was outfitted with a standard electrospray ionization (ESI)  
238 source, and data was acquired in negative mode with the voltage set to +4.4kV. Data were  
239 collected with an ion accumulation time of 0.3 sec from 98 – 900 m/z at 4M. One hundred  
240 forty-four scans were co-added. BrukerDaltonik (version 4.2) was used to convert raw spectra  
241 to a list of m/z values by applying FTMS peak picker module. Chemical formulas were then  
242 assigned using in-house software following the Compound Identification Algorithm<sup>46-49</sup>, using  
243 the criteria previously described by Graham et al.<sup>10,11</sup>. The chemical character of the compounds  
244 identified in the FTICR-MS spectrum and their biochemical classes were evaluated using Van  
245 Krevelen diagrams.

246 We calculated the  $\Delta G^{\circ}_{\text{COX}}$  to evaluate relationships between aerobic respiration and OM  
247 thermodynamics, as per LaRowe and Van Cappellen<sup>28</sup>. An expanded description of sample  
248 preparation, instrument and FTICR-MS data processing for estimating Van Krevelen diagrams  
249 and  $\Delta G^{\circ}_{\text{COX}}$  is presented in the Supplementary Methods.

### 250 **Identification of biochemical transformations using FTICR-MS**

251 Biochemical transformations were inferred by calculating all possible pairwise mass differences  
252 within a sample's spectrum and matching differences (within 1 ppm) to a list of common

253 biochemical transformations<sup>50</sup>. Biochemical transformations were identified following the  
254 procedures described by Breitling et al.<sup>50</sup> and previously employed by Bailey et al.<sup>34</sup>, Graham et  
255 al.<sup>10,11</sup>, Moritz et al.<sup>36</sup>, Kaling et al.<sup>35</sup>, and Stegen et al.<sup>12</sup>. Briefly, pairwise mass differences  
256 between all m/z peaks in a sample were compared with a reference list of 1298 commonly  
257 observed biochemical reactions of organic matter (Supplementary Table 2). For mass differences  
258 matching to compounds in the reference list, we inferred the gain or loss of that compound via a  
259 biochemical transformation.

## 260 **Statistical analyses**

261 All statistical analyses were completed using R (version 3.4.1). Linear regressions were used to  
262 assess the relationship between respiration rates and  $\overline{\Delta G^{\circ}_{\text{Cox}}}$ . Differences across groups were  
263 evaluated with one-sided Mann-Whitney U test. Permutational multivariate analysis of variance  
264 (PERMANOVA) of Bray–Curtis distances was used to assess dissimilarities among  
265 biogeochemical transformations in the “vegan” R package. PERMANOVAs were stratified by  
266  $\Delta G^{\circ}_{\text{Cox}}$  to account for any differences due to the thermodynamic properties of the treatment  
267 solution. Biochemical transformations were visualized with non-metric multidimensional scaling  
268 (NMDS).

269

270 **References**

- 271 1 Battin, T. J. *et al.* Biophysical controls on organic carbon fluxes in fluvial networks.  
272 *Nature geoscience* **1**, 95 (2008).
- 273 2 Cole, J. J. *et al.* Plumbing the global carbon cycle: integrating inland waters into the  
274 terrestrial carbon budget. *Ecosystems* **10**, 172-185 (2007).
- 275 3 Tranvik, L. J. *et al.* Lakes and reservoirs as regulators of carbon cycling and climate.  
276 *Limnology and Oceanography* **54**, 2298-2314 (2009).
- 277 4 Sawakuchi, H. O. *et al.* Carbon dioxide emissions along the lower Amazon River.  
278 *Frontiers in Marine Science* **4**, 76 (2017).
- 279 5 Raymond, P. A. *et al.* Global carbon dioxide emissions from inland waters. *Nature* **503**,  
280 355 (2013).
- 281 6 Ruhala, S. S. & Zarnetske, J. P. Using in-situ optical sensors to study dissolved organic  
282 carbon dynamics of streams and watersheds: A review. *Sci Total Environ* **575**, 713-723,  
283 doi:10.1016/j.scitotenv.2016.09.113 (2017).
- 284 7 Naegeli, M. W. & Uehlinger, U. Contribution of the hyporheic zone to ecosystem  
285 metabolism in a prealpine gravel-bed-river. *Journal of the North American Benthological*  
286 *Society* **16**, 794-804 (1997).
- 287 8 Battin, T. J., Kaplan, L. A., Newbold, J. D. & Hendricks, S. P. A mixing model analysis  
288 of stream solute dynamics and the contribution of a hyporheic zone to ecosystem  
289 function. *Freshwater Biology* **48**, 995-1014 (2003).
- 290 9 Kaplan, L. A., Wiegner, T. N., Newbold, J., Ostrom, P. H. & Gandhi, H. Untangling the  
291 complex issue of dissolved organic carbon uptake: a stable isotope approach. *Freshwater*  
292 *Biology* **53**, 855-864 (2008).

- 293 10 Graham, E. B. *et al.* Multi 'omics comparison reveals metabolome biochemistry, not  
294 microbiome composition or gene expression, corresponds to elevated biogeochemical  
295 function in the hyporheic zone. *Sci Total Environ* **642**, 742-753,  
296 doi:10.1016/j.scitotenv.2018.05.256 (2018).
- 297 11 Graham, E. B. *et al.* Carbon Inputs From Riparian Vegetation Limit Oxidation of  
298 Physically Bound Organic Carbon Via Biochemical and Thermodynamic Processes.  
299 *Journal of Geophysical Research: Biogeosciences* **122**, 3188-3205,  
300 doi:10.1002/2017jg003967 (2017).
- 301 12 Stegen, J. C. *et al.* Influences of organic carbon speciation on hyporheic corridor  
302 biogeochemistry and microbial ecology. *Nat Commun* **9**, 585, doi:10.1038/s41467-018-  
303 02922-9 (2018).
- 304 13 Regnier, P. *et al.* Anthropogenic perturbation of the carbon fluxes from land to ocean.  
305 *Nature geoscience* **6**, 597 (2013).
- 306 14 Butman, D. & Raymond, P. A. Significant efflux of carbon dioxide from streams and  
307 rivers in the United States. *Nature Geoscience* **4**, 839 (2011).
- 308 15 Hedin, L. O. *et al.* Thermodynamic constraints on nitrogen transformations and other  
309 biogeochemical processes at soil-stream interfaces *Ecology* **79**, 684-703,  
310 doi:10.1890/0012-9658(1998)079[0684:tconao]2.0.co;2 (1998).
- 311 16 McClain, M. E. *et al.* Biogeochemical hot spots and hot moments at the interface of  
312 terrestrial and aquatic ecosystems. *Ecosystems* **6**, 301-312 (2003).
- 313 17 Craig, L., Bahr, J. M. & Roden, E. E. Localized zones of denitrification in a floodplain  
314 aquifer in southern Wisconsin, USA. *Hydrogeology Journal* **18**, 1867-1879,  
315 doi:10.1007/s10040-010-0665-2 (2010).

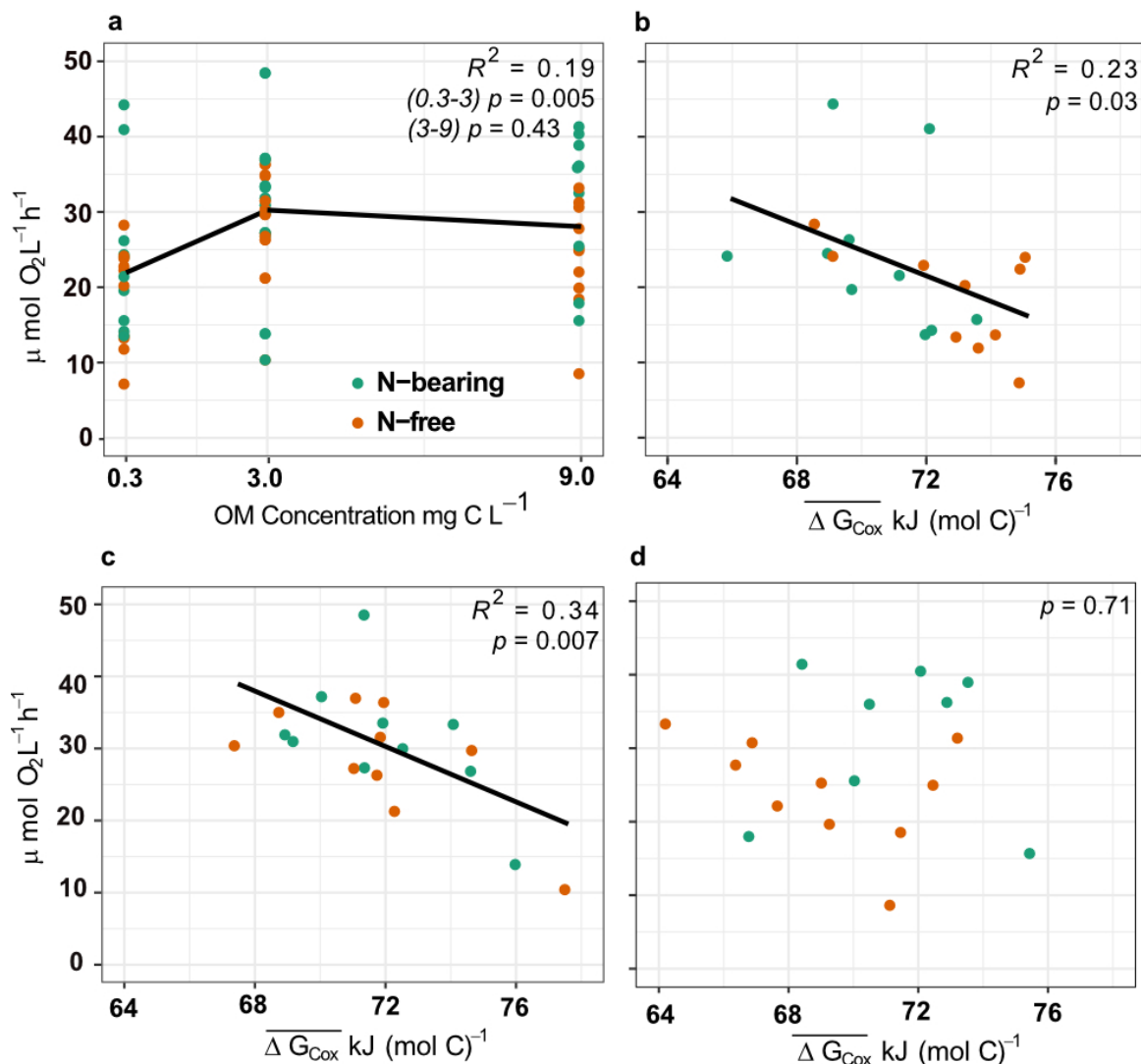
- 316 18 Jin, Q. & Bethke, C. M. A new rate law describing microbial respiration. *Appl. Environ.*  
317 *Microbiol.* **69**, 2340-2348 (2003).
- 318 19 Keiluweit, M., Nico, P. S., Kleber, M. & Fendorf, S. Are oxygen limitations under  
319 recognized regulators of organic carbon turnover in upland soils? *Biogeochemistry* **127**,  
320 157-171, doi:10.1007/s10533-015-0180-6 (2016).
- 321 20 Burd, A. B. *et al.* Terrestrial and marine perspectives on modeling organic matter  
322 degradation pathways. *Global change biology* **22**, 121-136 (2016).
- 323 21 Li, L. *et al.* Expanding the role of reactive transport models in critical zone processes.  
324 *Earth-science reviews* **165**, 280-301 (2017).
- 325 22 Boye, K. *et al.* Thermodynamically controlled preservation of organic carbon in  
326 floodplains. *Nature Geoscience* **10**, 415-419, doi:10.1038/ngeo2940 (2017).
- 327 23 Pracht, L. E., Tfaily, M. M., Ardissono, R. J. & Neumann, R. B. Molecular  
328 characterization of organic matter mobilized from Bangladeshi aquifer sediment: tracking  
329 carbon compositional change during microbial utilization. *Biogeosciences* **15**, 1733-1747,  
330 doi:10.5194/bg-15-1733-2018 (2018).
- 331 24 Musolff, A. *et al.* Spatio-temporal controls of dissolved organic carbon stream water  
332 concentrations. *Journal of Hydrology* **566**, 205-215, doi:10.1016/j.jhydrol.2018.09.011  
333 (2018).
- 334 25 Yang, Q., Zhang, X., Xu, X. & Asrar, G. R. An analysis of terrestrial and aquatic  
335 environmental controls of riverine dissolved organic carbon in the conterminous United  
336 States. *Water* **9**, 383 (2017).
- 337 26 Egli, T., Lendenmann, U. & Snozzi, M. Kinetics of microbial growth with mixtures of  
338 carbon sources. *Antonie van Leeuwenhoek* **63**, 289-298 (1993).



- 339 27 Zinn, M., Witholt, B. & Egli, T. Dual nutrient limited growth: models, experimental  
340 observations, and applications. *Journal of biotechnology* **113**, 263-279 (2004).
- 341 28 LaRowe, D. E. & Van Cappellen, P. Degradation of natural organic matter: A  
342 thermodynamic analysis. *Geochimica et Cosmochimica Acta* **75**, 2030-2042,  
343 doi:10.1016/j.gca.2011.01.020 (2011).
- 344 29 Berggren, M. & del Giorgio, P. A. Distinct patterns of microbial metabolism associated  
345 to riverine dissolved organic carbon of different source and quality. *Journal of*  
346 *Geophysical Research: Biogeosciences* **120**, 989-999, doi:10.1002/2015jg002963 (2015).
- 347 30 Sundh, I. Biochemical composition of dissolved organic carbon derived from  
348 phytoplankton and used by heterotrophic bacteria. *Appl. Environ. Microbiol.* **58**, 2938-  
349 2947 (1992).
- 350 31 Rosenstock, B. & Simon, M. Use of dissolved combined and free amino acids by  
351 planktonic bacteria in Lake Constance. *Limnology and Oceanography* **38**, 1521-1531  
352 (1993).
- 353 32 Khatoon, H., Solanki, P., Narayan, M., Tewari, L. & Rai, J. Role of microbes in organic  
354 carbon decomposition and maintenance of soil ecosystem. (2017).
- 355 33 Arnosti, C. *et al.* Extracellular enzymes in terrestrial, freshwater, and marine  
356 environments: perspectives on system variability and common research needs.  
357 *Biogeochemistry* **117**, 5-21 (2014).
- 358 34 Bailey, V. L., Smith, A., Tfaily, M., Fansler, S. J. & Bond-Lamberty, B. Differences in  
359 soluble organic carbon chemistry in pore waters sampled from different pore size  
360 domains. *Soil Biology and Biochemistry* **107**, 133-143 (2017).

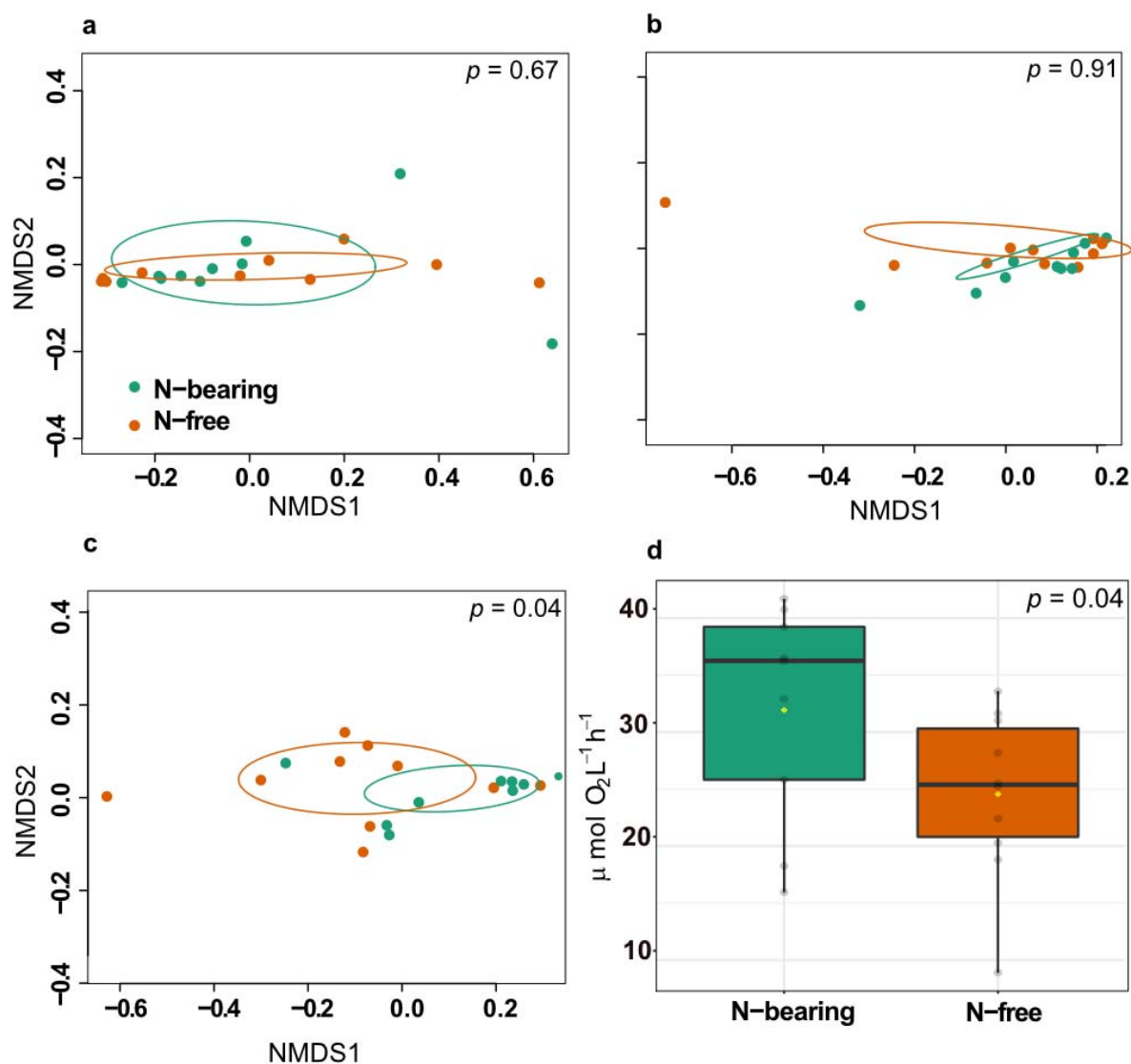
- 361 35 Kaling, M. *et al.* Mycorrhiza-triggered transcriptomic and metabolomic networks  
362 impinge on herbivore fitness. *Plant physiology* **176**, 2639-2656 (2018).
- 363 36 Moritz, F., Kaling, M., Schnitzler, J. P. & Schmitt-Kopplin, P. Characterization of poplar  
364 metabotypes via mass difference enrichment analysis. *Plant Cell Environ* **40**, 1057-1073,  
365 doi:10.1111/pce.12878 (2017).
- 366 37 Moorhead, D. L. & Sinsabaugh, R. L. A theoretical model of litter decay and microbial  
367 interaction. *Ecological Monographs* **76**, 151-174 (2006).
- 368 38 Treseder, K. K. Nitrogen additions and microbial biomass: A meta-analysis of  
369 ecosystem studies. *Ecology letters* **11**, 1111-1120 (2008).
- 370 39 Vitousek, P. M. & Howarth, R. W. Nitrogen limitation on land and in the sea: how can it  
371 occur? *Biogeochemistry* **13**, 87-115 (1991).
- 372 40 Wang, G., Post, W. M. & Mayes, M. A. Development of microbial-enzyme-mediated  
373 decomposition model parameters through steady-state and dynamic analyses. *Ecological*  
374 *Applications* **23**, 255-272 (2013).
- 375 41 Sulman, B. N., Phillips, R. P., Oishi, A. C., Shevliakova, E. & Pacala, S. W. Microbe-  
376 driven turnover offsets mineral-mediated storage of soil carbon under elevated CO<sub>2</sub>.  
377 *Nature Climate Change* **4**, 1099 (2014).
- 378 42 Vachon, D., Prairie, Y. T., Guillemette, F. & Del Giorgio, P. A. Modeling allochthonous  
379 dissolved organic carbon mineralization under variable hydrologic regimes in boreal  
380 lakes. *Ecosystems* **20**, 781-795 (2017).
- 381 43 Brookshire, E. N. J., Valett, H. M., Thomas, S. A. & Webster, J. R. Coupled cycling of  
382 dissolved organic nitrogen and carbon in a forest stream. *Ecology* **86**, 2487-2496 (2005).

- 383 44 Bernal, S., Lupon, A., Catalán, N., Castelar, S. & Martí, E. Decoupling of dissolved  
384 organic matter patterns between stream and riparian groundwater in a headwater forested  
385 catchment. *Hydrology and Earth System Sciences* **22**, 1897-1910, doi:10.5194/hess-22-  
386 1897-2018 (2018).
- 387 45 Goldman, A. E. *et al.* Biogeochemical cycling at the aquatic–terrestrial interface is linked  
388 to parafluvial hyporheic zone inundation history. *Biogeosciences* **14**, 4229-4241,  
389 doi:10.5194/bg-14-4229-2017 (2017).
- 390 46 Kujawinski, E. B. & Behn, M. D. Automated analysis of electrospray ionization Fourier  
391 transform ion cyclotron resonance mass spectra of natural organic matter. *Analytical*  
392 *Chemistry* **78**, 4363-4373 (2006).
- 393 47 Minor, E. C., Steinbring, C. J., Longnecker, K. & Kujawinski, E. B. Characterization of  
394 dissolved organic matter in Lake Superior and its watershed using ultrahigh resolution  
395 mass spectrometry. *Organic geochemistry* **43**, 1-11 (2012).
- 396 48 Tfaily, M. M. *et al.* Sequential extraction protocol for organic matter from soils and  
397 sediments using high resolution mass spectrometry. *Analytica chimica acta* **972**, 54-61  
398 (2017).
- 399 49 Tolić, N. *et al.* Formularity: software for automated formula assignment of natural and  
400 other organic matter from ultrahigh-resolution mass spectra. *Analytical chemistry* **89**,  
401 12659-12665 (2017).
- 402 50 Breitling, R., Ritchie, S., Goodenowe, D., Stewart, M. L. & Barrett, M. P. Ab initio  
403 prediction of metabolic networks using Fourier transform mass spectrometry data.  
404 *Metabolomics* **2**, 155-164, doi:10.1007/s11306-006-0029-z (2006).



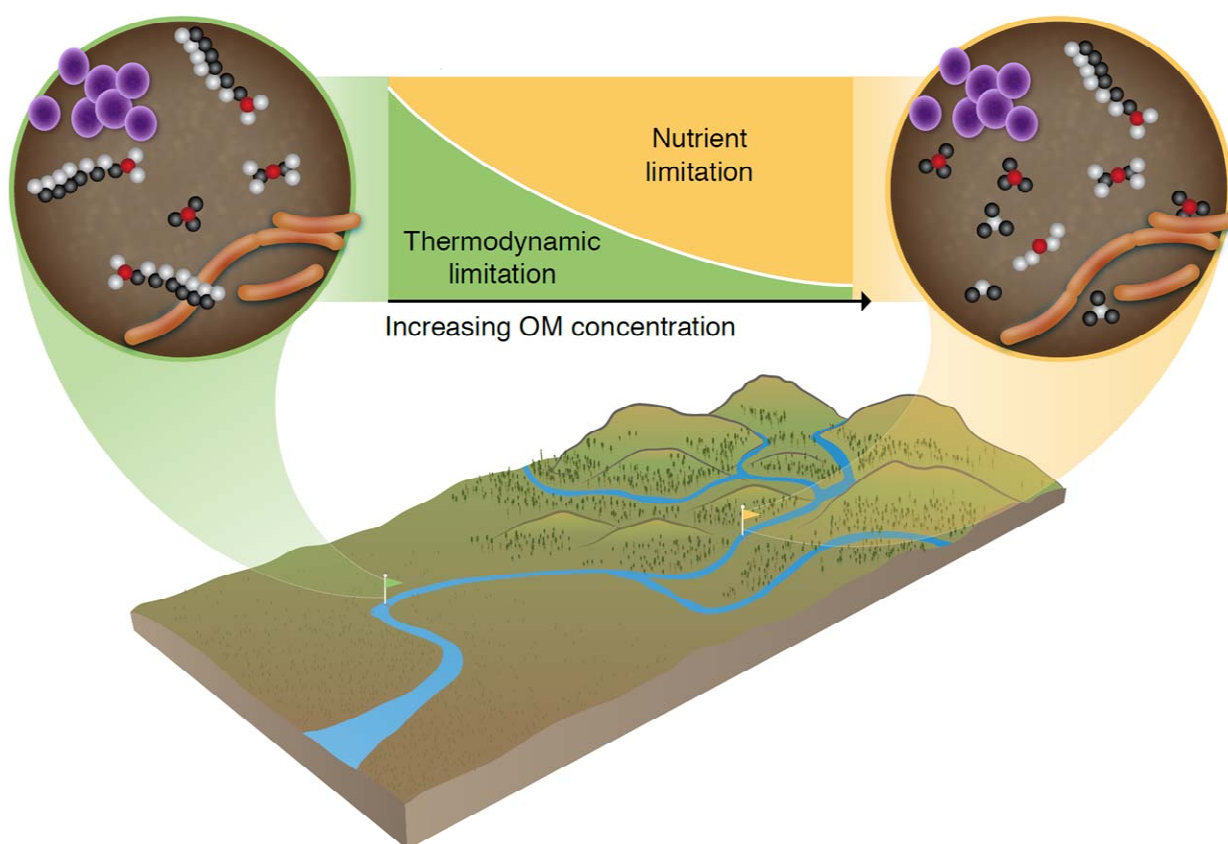
405

406 **Fig. 1** Aerobic respiration rates in microcosms and its relationship with  $\overline{\Delta G^{\circ}_{\text{Cox}}}$ . (a) Respiration  
 407 rates were higher in microcosms amended with 3  $\text{mg C L}^{-1}$  vs. 0.3  $\text{mg C L}^{-1}$ , while microcosms  
 408 receiving 3  $\text{mg C L}^{-1}$  and 9  $\text{mg C L}^{-1}$  had similar respiration rates, indicating carbon limitation at  
 409 low concentrations of amended OM that was alleviated with increasing OM addition. In  
 410 microcosms with OM added at (b) 0.3  $\text{mg C L}^{-1}$  and (c) 3  $\text{mg C L}^{-1}$ ,  $\overline{\Delta G^{\circ}_{\text{Cox}}}$  shows a negative  
 411 relationship with respiration, while microcosms with (d) 9  $\text{mg C L}^{-1}$  amendments show no  
 412 relationship between OM thermodynamics and respiration rates.



413

414 **Fig. 2** Biochemical transformations between N-bearing and N-free OM amendments and its link  
415 with respiration rates. Non-metric multidimensional scaling (NMDS) plots of microcosms  
416 receiving low OM concentrations (a) 0.3 mg C L<sup>-1</sup> and (b) 3 mg C L<sup>-1</sup> showed no difference in  
417 biochemical transformation profiles between N-bearing and N-free amendments. In contrast,  
418 microcosms receiving high OM concentrations (c) 9 mg C L<sup>-1</sup> had significantly different  
419 biochemical transformation profiles between N-bearing and N-free amendments. (d) Microcosms  
420 amended with N-bearing OM at 9 mg C L<sup>-1</sup> also showed enhanced respiration vs. those receiving  
421 N-free OM at the same concentration. In contrary, respiration rates were not statistically different  
422 between N-bearing and N-free microcosms receiving low OM (0.3 and 3 mg C L<sup>-1</sup>). Colors in  
423 all panels indicate N-bearing (teal) and N-free (orange) OM amendments. *P*-values in (a-c) were  
424 derived from PERMANOVAs, and the *p*-value in (d) was calculated using a one-sided Mann-  
425 Whitney U test.



426

427 **Fig. 3** Conceptualization of thermodynamic and nutrient regulations on aerobic respiration. We  
428 propose a new conceptual model in which thermodynamic and nutrient limitations dually control  
429 aerobic respirations. We suggest that thermodynamic properties of OM govern aerobic  
430 respiration rates in ecosystems with low carbon to nutrient ratios. When OM concentration  
431 reaches a threshold, thermodynamic controls do not persist, and nutrient availability, particularly  
432 N regulate respiration. This work highlights a structural gap in aquatic biogeochemical models  
433 and challenges long-held beliefs about aerobic metabolism being solely governed by reaction  
434 kinetics. This new paradigm provides a link between OM chemistry and biogeochemical rates  
435 with direct avenues for model incorporation, where OM chemistry regulates OM oxidation  
436 through its thermodynamic properties until OM concentrations are sufficient to induce nutrient  
437 limitations.

438